Hybrid spectral CT system with clinical rapid kVp-switching x-ray tube and dual-layer detector for improved iodine quantification

Olivia F. Sandvold[a,b], **Roland Proksa**[a], **Heiner Daerr**[c], **Amy E. Perkins**[d], **Kevin M. Brown**[d], **Nadav Shapira**[a], **Thomas Koehler**[c], **J. Webster Stayman**[e], **Grace J. Gang**[a], **Ravindra M. Manjeshwar**[d], **Peter B. Noël**[a]

[a]Department of Radiology, Perelman School of Medicine, Philadelphia, USA 19104

[b]Department of Bioengineering, University of Pennsylvania, Philadelphia, USA 19104

[c]Philips Innovative Technologies, Hamburg, Germany 22335

[d]Philips Healthcare, Cleveland, USA 44122

[e]Johns Hopkins University, Baltimore, USA 21218

Abstract

Spectral computed tomography (CT) is a powerful diagnostic tool offering quantitative material decomposition results that enhance clinical imaging by providing physiologic and functional insights. Iodine, a widely used contrast agent, improves visualization in various clinical contexts. However, accurately detecting low-concentration iodine presents challenges in spectral CT systems, particularly crucial for conditions like pancreatic cancer assessment. In this study, we present preliminary results from our hybrid spectral CT instrumentation which includes clinical-grade hardware (rapid kVp-switching x-ray tube, dual-layer detector). This combination expands spectral datasets from two to four channels, wherein we hypothesize improved quantification accuracy for low-dose and low-iodine concentration cases. We modulate the system duty cycle to evaluate its impact on quantification noise and bias. We evaluate iodine quantification performance by comparing two hybrid weighting strategies alongside rapid kVp-switching. This evaluation is performed with a polyamide phantom containing seven iodine inserts ranging from 0.5 to 20 mg/mL. In comparison to alternative methodologies, the maximum separation configuration, incorporating data from both the 80 kVp, low photon energy detector layer and the 140 kVp, high photon energy detector layer produces spectral images containing low quantitative noise and bias. This study presents initial evaluations on a hybrid spectral CT system, leveraging clinical hardware to demonstrate the potential for enhanced precision and sensitivity in spectral imaging. This research holds promise for advancing spectral CT imaging performance across diverse clinical scenarios.

Keywords

Dual-energy CT; spectral CT; quantitative imaging; CT instrumentation; imaging systems; iodine contrast

1. INTRODUCTION

Spectral computed tomography (CT) generates quantitative material decomposition results that increase CT diagnostic utility in clinical settings through additional physiologic and functional information[1]. Iodine stands as the prevailing choice among CT contrast agents, consistently employed to enhance visualization across a spectrum of anatomical regions and pathological conditions. A demand arises for increased sensitivity towards the presence of low-concentration iodine within the framework of current spectral CT systems. This necessity is particularly evident in scenarios such as pancreatic cancer assessments, wherein the dense stroma surrounding both parenchymal and vascular structures limits enhancement causing challenges to accurately determine the iodine signal[2,3]. Furthermore, this sensitivity gap is notable in the pediatric demographic due to their reduced bolus requirements and stringent dosage constraints, as well as in adults with a heightened susceptibility to kidney injuries stemming from contrast administration. The ability to accurately measure low concentration iodine is further degraded in ultra-low radiation dose settings as increased noise may create a bias in spectral results. Thus, it is important to optimize spectral CT instrumentation to have high iodine sensitivity while minimizing radiation dose levels.

There are several technological approaches to enable spectral CT[4]. Currently, clinical spectral CT systems are available with multi-energy capabilities through use of either a dual-source geometry, rapid kVp-switching (kVp-s) x-ray tube, spectral detectors (both energy integrating and photon-counting), or with use of spectral spatial filters. When evaluating various implementations of spectral CT, it becomes evident that no single solution encompasses all the benefits. As a result, each approach presents its own set of advantages and disadvantages, particularly in terms of factors such as spectral separation, susceptibility to motion artifacts, seamless clinical integration, etc.

To overcome these technical obstacles, we propose a **hybrid spectral CT instrumentation** combining a clinical **dual-layer spectral detector** with a clinical-grade **rapid kVp-s tube**. This doubles the number of spectral channels available in a single acquisition from two to four. As material decomposition with four input channels is computationally much more demanding than one with two input channels, and in order to maintain the current spectral pre-processing pipeline, we investigate different ways to combine the four channels into two before decomposition. These weighting schemes represent varying amounts of photon data incorporated in the final spectral images. We hypothesize the additional spectral diversity from the combination of tube voltage and layer pairs will generate more accurate and less noisy quantification results necessary for low dose and low iodine concentration clinical cases[5]. Availability of spectrally diverse channels will further enable us to optimize material decomposition based on patient habitus, dose requirements, and clinical need.

In this study, we present the preliminary findings from our hybrid spectral CT instrumentation. Our investigation centers around the assessment of iodine quantification performance. To achieve this, we compare the efficacy of rapid kVp-switching alongside two distinct hybrid weighting schemes at three radiation exposure duty cycles and three rotation speeds.

2. METHODS

The hybrid spectral CT benchtop (Fig. 1A), equipped with a clinical dual-layer energy integrating detector and clinical-grade rapid kVp-switching x-ray tube (Philips Healthcare), was operated at 570 mA in switching mode alternating between 140 and 80 kVp. For each tube voltage there are two paired projections with unique energy spectra captured in the dual-layer detector. These four projections, also referenced as channels, are identified by a kVp_{Layer} label as depicted in Fig. 1B. Note, the upper detector layer contains low energy (LowE) photon projection data, and the lower detector layer contains high energy (HighE) photon information. A polyamide (PA6) 270 mm diameter cylindrical phantom containing eight tissue-mimicking inserts (iodine 0.5, 1.0, 2.0, 5.0, 10.0, 15.0, 20.0 mg/mL and solid water, Sun Nuclear) was rotated at a rotation frequency of 1 Hz. Three duty cycles (15/85, 33/67, 75/25) were used to investigate how different partitioning of the total scan time between 140 kVp and 80 kVp impacts the quantitative performance. This produced three different patient radiation doses since the tube current, total number of paired projections (1000), and scan time (1 s) were fixed and tube flux is higher at 140 kVp than at 80 kVp at the same current. For this system, the minimum cycle time, or total amount of time for high and low kVp, was 200 μs and the minimum integration period (IP), or duration of an individual high or low kVp period was 100 μs. The phantom distance from the source was 570 mm. Beam collimation was set to a width of 16 slices (10 mm).

Photoelectric effect, scatter, iodine density, and virtual non-contrast images were generated with a processing pipeline using a projection-based 2D material decomposition. The basis functions for the 2D material decomposition were estimated with a physical system model and a fast reference detector on the bench for dynamic flux calibration. We investigated the impact of spectral diversity and dose utilization on material decomposition by reconstructing combinations of channels to generate two new spectral input channels. The weights of the three selected combinations are defined in Table 1 with the input variable representing the summation of the product of weights and detector reading energies for each kVp_{Layer}. For example, to perform the kVp-switching reconstruction, we treat the dual-layer detector as a single layer energy-integrating detector by summing the detector signals from both layers for each kVp cycle. The "max separation" scheme, in contrast, uses the least number of spectral channels but contains the highest spectral separation between material decomposition inputs. No additional denoising was applied to the images.

Measurements were taken from regions of interest (ROIs) placed on each insert in each image and in the background phantom material to measure the mean and standard deviation (noise) in the iodine concentration values in iodine density images in each of the 16 slices (Fig. 2). Quantitative iodine bias, or nominal error, was calculated by taking the difference between the mean concentration in each ROI and the expected rod concentration in mg/mL.

3. RESULTS

In our investigation regarding the impact of duty cycle ratio (140 kVp / 80 kVp) on noise in spectral images, we observed notable differences. Specifically, when considering the duty cycle ratios of 15/85, 33/67, and 75/25 at a phantom rotation frequency of 1 Hz, the

average noise in the background ROI was smallest for the 33/67 duty cycle max separation weighting scheme across all duty cycles and weighting schemes and that the maximum separation scheme outperformed kVp-switching regardless of duty cycle ratio (Fig. 3).

In 33/67 duty cycle, the maximum separation and "all 80/highE 140" weighting schemes contained the same lowest mean iodine density noise values at 0.52 mg/mL in the background ROI. Background noise was higher in the 15/85 and 75/25 duty cycle ratio acquisitions compared to the 33/67 results for the same weighting schemes. In the kVp-s weighting scheme, there was a 33% increase in noise comparing the 33/67 duty cycle average noise to the 75/25 kVp-s average noise. Within each duty cycle, the maximum separation had the smallest noise compared to the other two weighting schemes except in the 33/67 duty cycle where the max separation and all "80/highE 140" scheme contained the same average background noise in the iodine density images. The kVp-s scheme produced the highest amount of noise with averages of 0.65, 0.59, and 0.79 mg/mL in the background ROI for the 15/85, 33/67, and 75/25 duty cycles respectively.

In the 15/85 and 33/67 duty cycles, the average bias in the selected rods for all three weighting schemes was below 0.5 mg/mL. The lowest iodine density error on average was captured in the 15/85 and 33/67 duty cycle ratio acquisitions with the maximum separation weighting scheme at 0.07 and 0.15 mg/mL respectively on average in the selected rods (Fig. 4). The smallest average bias in the 75/25 duty cycle scan was using the "all 80/highE 140" kVp scheme which produced an average error of −0.36 mg/mL across the selected iodine inserts. In contrast to 15/85 and 33/67 duty cycles, the 75/25 duty cycle acquisitions caused an underestimation of iodine density for all three weighting schemes. This selected duty cycle contained the least balanced detector signal-to-noise ratios between 140 and 80 kVp tube voltages with 140 kVp dominating the majority of the scan acquisition. Therefore, it was expected that this duty cycle resulted in the largest magnitude error of the tested duty cycles.

4. DISCUSSION

To the best of our knowledge, this is one of the first reports of using clinical-grade x-ray source and detector technology to illustrate the potential of hybrid spectral CT systems. Our findings underscore the advantages of leveraging projection data with spectral diversity, as evidenced by the noise reduction and minimal iodine bias observed in iodine density images across the iodine inserts. In comparison to alternative methodologies, the "max separation" configuration stands out, incorporating data from both the 80 kVp, low photon energy detector layer and the 140 kVp, high photon energy detector layer. Additionally, we demonstrate the importance of selection of an appropriate duty cycle ratio for the rapid kVp-switching tube. With the 15/85 duty cycle ratio, the max separation scheme resulted in an average iodine bias of less than 0.1 mg/mL compared to the 75/25 duty cycle where the "all 80/highE 140 kVp" scheme had the smallest average bias across schemes of −0.36 mg/mL. In future evaluations we will present results from a reconstruction with a four-input channel material decomposition. Furthermore, we hypothesize that specialized spectral weighting schemes may provide advantages. In order to achieve maximally reduced

noise and improved spectral quantitative accuracy, we will investigate more complex optimal weighting reconstruction strategies. We will also expand studied patient habitus sizes.

5. CONCLUSION

In this study, we demonstrate the feasibility of a hybrid spectral CT system utilizing a clinical kVp-switching tube and a clinical dual-layer spectral detector. Based on a comparison of material decomposition performance, we demonstrate that an additional spectral diversity resulting from the combination of these technologies improves quantitative accuracy and reduces noise in the basis images.

ACKNOWLEDGEMENTS

REFERENCES

1. Mccollough CH, Boedeker K, Cody D, Duan X, Flohr T, Halliburton SS, Hsieh J, Layman RR, Pelc NJ. Principles and applications of multienergy CT: Report of AAPM Task Group 291. Medical Physics. 2020;47(7). doi: 10.1002/mp.14157.

2. Mankoff DA, Dunnwald LK, Partridge SC, Specht JM. Blood flow-metabolism mismatch: good for the tumor, bad for the patient. Clin Cancer Res. 2009;15(17):5294–6. Epub 20090825. doi: 10.1158/1078-0432.Ccr-09-1448. [PubMed: 19706819]

3. Xie D, Xie K. Pancreatic cancer stromal biology and therapy. Genes Dis. 2015;2(2):133–43. doi: 10.1016/j.gendis.2015.01.002. [PubMed: 26114155]

4. Sellerer T, Noel PB, Patino M, Parakh A, Ehn S, Zeiter S, Holz JA, Hammel J, Fingerle AA, Pfeiffer F, Maintz D, Rummeny EJ, Muenzel D, Sahani DV. Dual-energy CT: a phantom comparison of different platforms for abdominal imaging. Eur Radiol. 2018;28(7):2745–55. Epub 20180205. doi: 10.1007/s00330-017-5238-5. [PubMed: 29404773]

5. Tivnan M, Wang W, Gang GJ, Liapi E, Noël PB, Stayman JW, editors. Combining spectral CT acquisition methods for high-sensitivity material decomposition. Medical Imaging 2020: Physics of Medical Imaging; 2020 2020–03-16: SPIE. doi: 10.1117/12.2550025.
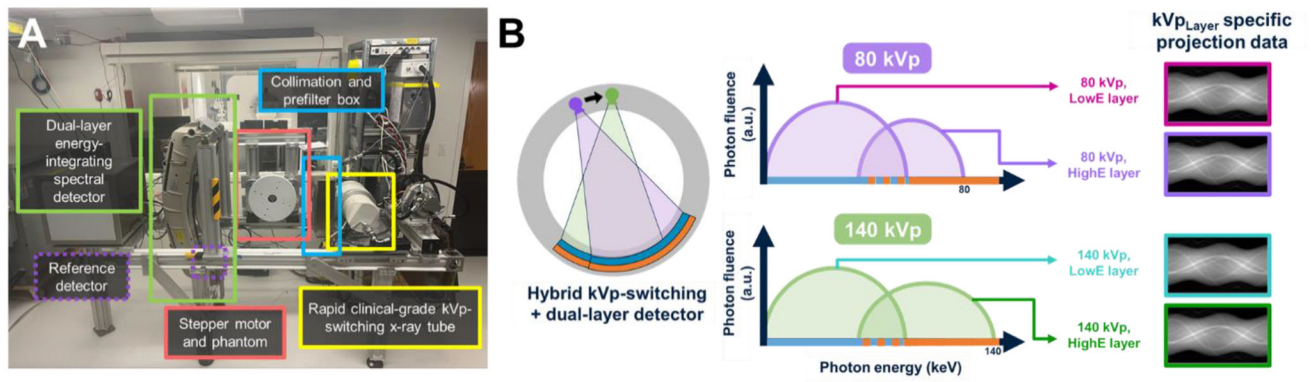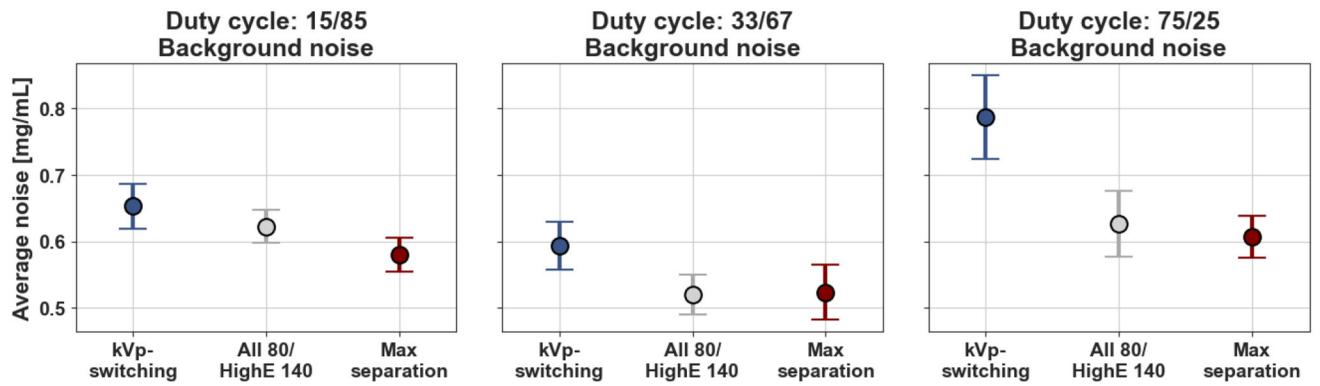
Figure 1.

(A) Photograph of CT bench and labeled components. (B) Schematic depicting the hybrid CT system combining spectral technologies and the resulting four projection data channels for each kVp and each layer in a single acquisition.
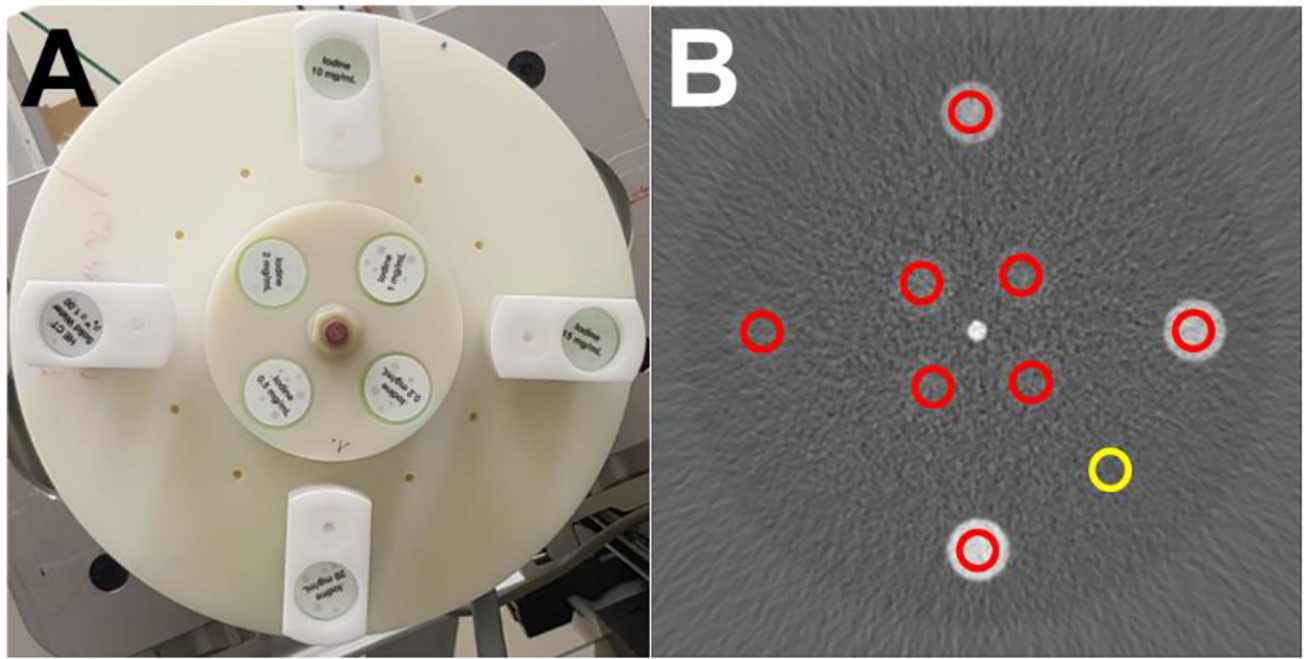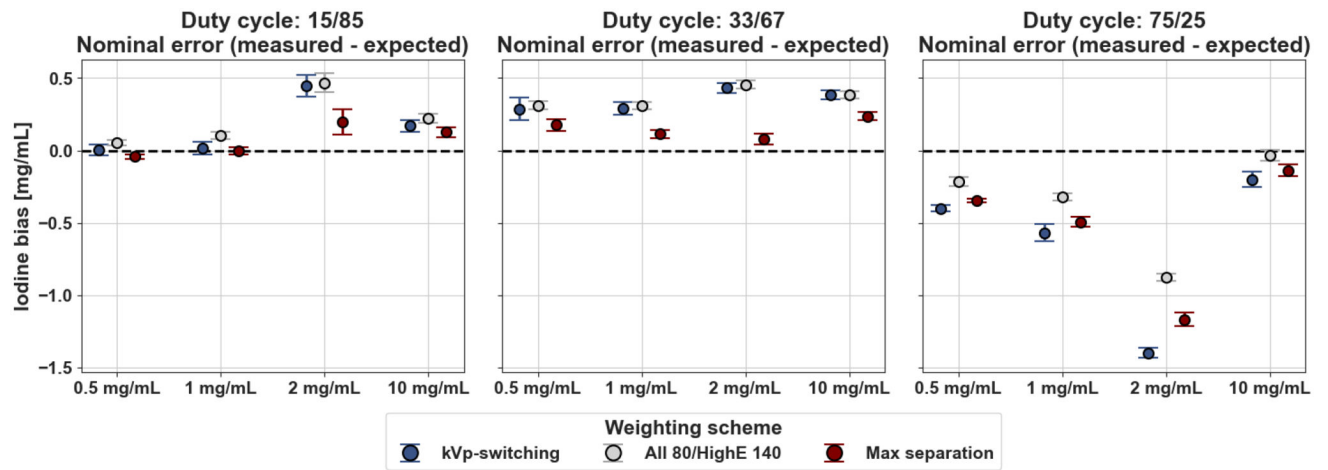
Figure 2.
(A) Photograph of polyamide phantom with inserts. (B) Iodine density image of kVp-s recon with insert ROIs (red) and the background ROI (yellow). WL: 5 WW: 50 mg/mL Iodine.

Figure 3.
Comparison of mean iodine density noise across the 16 slices in the background ROI for the three material decomposition weighting schemes within each duty cycle ratio. The maximum separation scheme contained the lowest amount of noise in each of the selected duty cycle ratios.

Figure 4.

Mean iodine density bias across the 16 slices in selected iodine inserts for the three material decomposition weighting schemes within each duty cycle ratio. The maximum separation scheme contained the lowest bias for both 15/85 and 33/67 duty cycles while "all 80/highE 140" scheme contained the lowest iodine bias in the 75/25 duty cycle ratio scan.

Table 1:

Weighting equation and weights to combine projections raw data into two new data channels.

Input $= W_{80,lowE} \times 80\,kVp_{lowE} + W_{80,highE} \times 80\,kVp_{highE} + W_{140,lowE} \times 140\,kVp_{lowE} + W_{140,highE} \times 140\,kVp_{highE}$											
	kVp-switching				"All 80/HighE 140" LowE + HighE 80 kVp/HighE 140 kVp				"Max separation" LowE 80 kVp/HighE 140 kVp			
	$W_{80,lowE}$	$W_{80,highE}$	$W_{140,lowE}$	$W_{140,highE}$	$W_{80,lowE}$	$W_{80,highE}$	$W_{140,lowE}$	$W_{140,highE}$	$W_{80,lowE}$	$W_{80,highE}$	$W_{140,lowE}$	$W_{140,highE}$
Input 1	**1.0**	**1.0**	0	0	**1.0**	**1.0**	0	0	**1.0**	0	0	0
Input 2	0	0	**1.0**	**1.0**	0	0	0	**1.0**	0	0	0	**1.0**